Application of chemical exchange saturation transfer (CEST) in neuroimaging

Kahina El Mamoune, Laurent Barantin, Hans Adriaensen, Yves Tillet

Application of Chemical Exchange Saturation Transfer (CEST) in neuroimaging.

Kahina El Mamoune[1,2,5], Laurent Barantin[4,5], Hans Adriaensen[1,3,5], Yves Tillet[1,5]

1 Physiologie de la Reproduction et des Comportements, UMR 085 INRAE, CNRS 7247, Université de Tours, IFCE, Centre INRAE Val de Loire, 37380 Nouzilly France
2 Siemens Healthcare SAS, Saint Denis, France
3 CIRE UMR 085 INRAE, CNRS 7247, Université de Tours, IFCE, Centre INRAE Val de Loire, 37380 Nouzilly France
4 iBrain, UMR 1253 INSERM, Université de Tours, 10 Bd Tonnellé - 37032 Tours France
5 SFR FED 4226, Université de Tours, 2 Bd Tonnellé - 37032 Tours France

Author for correspondance : Yves Tillet, Physiologie de la Reproduction et des Comportements, UMR 085 INRAE, CNRS 7247, Université de Tours, IFCE, Centre INRAE Val de Loire, 37380 Nouzilly France – yves.tillet@inrae.fr

Conflicts of Interest: The authors have no conflicts of interest to declare.

Keywords : MRI, in vivo neuroimaging, CEST contrast agent, chemical neuroanatomy

Abstract :

Since the early eighties MRI has become the most powerful technic for *in-vivo* imaging particularly in the field of brain research. This non-invasive method allows acute anatomical observations of the living brain similar to post-mortem dissected tissues. However, one of the main limitation of MRI is that it does not make possible the neurochemical identification of the tissues conversely to positron emission tomography scanner which can provide a specific molecular characterization of tissue, in spite of poor anatomical definition. To gain neurochemical information using MRI, new categories of contrast agents were developed from the beginning of the 2000's, particularly using the chemical-exchange saturation transfer (CEST) method. This method induces a significant change in the magnitude of the water proton signal and allows the detection of specific molecules within the tissues like sugars, amino acids, transmitters, and nucleosides. This short review presents several CEST contrast agents and their recent developments for *in vivo* detection of metabolites and neurotransmitters in the brain for research and clinical purposes.

Abbreviations

2DG	2-deoxy-D-glucose
2DG6P	2-deoxy-D-glucose-6-phosphate
ADP	Adenosine diphosphate
APT	Amide proton transfer
ATP	Adenosine Triphosphate
BBB	Blood Brain Barrier
CE-MRI	Contrast-Enhanced MRI
CEST	Chemical exchange saturation transfer
CrCEST	Creatine-based CEST
CT	Computerized Tomography
DGE	Dynamic Glucose Enhanced
DiaCEST	diamagnetic CEST
DWI	Diffusion Weighted Imaging
FDA	Food and Drug Administration
GluCEST	Glutamate-based CEST
GlucoCEST	Glucose-based CEST
LipoCEST	Liposome-based CEST
MICEST	Myo-inositol-based CEST
MRI	Magnetic Resonance Imaging
MRS	Magnetic Resonance Spectroscopy
NMR	Nuclear Magnetic Resonance
PARACEST	Paramagnetic CEST
PET	Positron-emission tomography
PWI	Perfusion Weighted Imaging
RF	Radio Frequency
rNOE	relayed Nuclear Overhauser Effect

Introduction

Since its invention in the 1970's, Magnetic Resonance Imaging (MRI) has quickly found its place in the medical field and *in vivo* research, particularly in neurobiology. Unlike Computerized Tomography (CT) using X rays, MRI can in a non-invasive and non-ionizing way visualize soft tissues. MRI principle consists in using a magnetic field (typically 1.5 or 3 Tesla in medicine applications), and applying a Radio-Frequency (RF) wave to excite or refocus in this case the protons of water molecules. These protons can absorb and emit radio-frequency energy informing on the water distribution in different tissues (Grover et al 2015). This technique generates high spatial resolution images in two or three dimensions. The contribution of MRI in neuroimaging is important since it allows to visualize brain tissues, its architecture as well as brain traumas, tumors, and gives an idea of the activity of the brain through functional MRI. Despite its ability to distinguish morphological and structural changes, in neurobiology, identification of different cellular populations or distribution of neurotransmitters in the brain is impossible. So far, metabolic or functional activity, including distribution of neurotransmitters are only possible using nuclear medicine imaging techniques after injection of a radioactive compound, despite its lower spatial resolution. The impossibility of being able to image a specific target lead to the development of specific contrast agents for MRI. Among the different types of contrast agents that have been developed, Chemical Exchange Saturation Transfer (CEST) contrast agents is found to be promising in both research and medicine (Sherry and Woods, 2008).

1 The Chemical Exchange Saturation Transfer (CEST) principle

The CEST effect makes possible the indirect detection of the presence of solute, which is not directly observable because of their too small quantity. It is based on the observation of the saturation transfer between 2 pools of protons in constant exchange (characterized by their exchange rates), the protons of free water (large pool) and the labile protons of the solute (small pool) (Figure 1A). A saturation radiofrequency pulse is applied to the resonant frequency of the labile protons of the solute (Figure 1B), which has the effect - due to their chemical exchange rate - of transferring part of the saturation to the pool of free protons of the water, resulting in a decrease in the NMR signal of free protons.

The detection of the CEST effect is linked to the exchange rate and also to the resonance frequency relative to water, to the pH, to temperature and to the magnetic field strength. The sensitivity of CEST contrast is higher than direct observation of these protons through Magnetic Resonance Spectroscopy (MRS), which permits also the visualization of specific molecules. Compared to MRS, CEST has a higher spatial resolution and sensitivity. Furthermore, the use of a selective saturation pulse frequency to saturate soluble protons allows the CEST contrast to be "switched on/off", leading CEST effect to be exploited as a novel and powerful contrast mechanism for MRI (Liu et al 2013; van Zijl et al, 2011), and enables the use of multiple CEST agents simultaneously for labeling.

In practice, it is necessary to measure and represent the normalized longitudinal magnetization of the pool of observable protons (water) as a function of the applied saturation frequency, generating a Z or CEST spectrum (Fig 1C). This representation thus highlights 2 minima: one relating to the direct saturation of the protons of water and one

observed at the saturation frequency of the solute. Another mode of representation is to overcome the direct contribution of water protons, through the representation of the asymmetric magnetization transfer ratio denoted MTRasym (Fig 1D).

Even if CEST imaging is a promising tool to study certain molecules, it suffers from methodological drawbacks. For example, CEST is very sensitive to B0 field inhomogeneities that shift the Larmor frequency. As a result, saturation pulses may be applied at a wrong offset, depending of spatial localization. One efficient way to correct this is to acquire an additional set of data with a finer sampling of the saturation pulses around the water signal, to estimate the effective Larmor frequency voxel by voxel (WASSR technique, Kim et al 2009).

Furthermore, as macromolecular effects are asymmetric and lipophilic peaks exist on the right side of the water peak, it is important to minimize these sources of error that may confound the measurements. Several techniques were proposed such as double frequency irradiation, lorentzian differences or lorentzian curve fitting (Zaiss et al 2011).

This technique permits to image several different classes of molecules. CEST contrast agents can be divided into two families: CEST with endogenous agents that are molecules naturally present in cells and CEST with exogenous chemical agents whose chemical structures can be very complex. Endogenous contrast agents are diamagnetic molecules of relatively small size which possess the property of being able to exchange protons via hydrogen exchange with water (amide (-NH), amine ($-NH_2$), hydroxyl (-OH) and guanidyl (-N $C=(NH_2)_2$) moieties) in a frequency-specific manner (chemical shift). These molecules have a slow exchange rate with a resonance frequency close to that of water. Molecules such as peptides, mobile cytosolic proteins, glucose, glutamate, myo-inositol and creatine were imaged to study the pathophysiology of neurological diseases and traumatic brain injuries (Tab.1). The exogenous contrast agents can be diamagnetic, thus relatively close to the structural and chemical properties of the endogenous molecules, or paramagnetic with a more complex structure containing a paramagnetic ion (lanthanide or transition metal). The paramagnetic agents are synthesized to possess a slow exchange rate but in opposition to diamagnetic molecules, these agents have a larger chemical shift from water that allows more selective saturation and exploitation of faster proton exchange rates (Zhou and van Zijl, 2006).

As we previously explained, CEST contrast is dependent on proton exchange rate, and is therefore inherently sensitive to pH, as pH-dependence of proton exchange is known since before the origin of CEST imaging in 2000. Importantly, the proton exchange rate is pH-sensitive for several types of exchangeable protons including amine and amide groups. Ward and Balaban firstly explained how to measure tissue pH with CEST agents and investigated its applications (Ward and Balaban, 2000).

The potential of CEST imaging has encouraged the development of a wide range of biomedical imaging applications and remains a rapidly growing field in the MR community. This review aims to show the different contrast agents using the CEST effect and their applications in neuroimaging.

2 Endogenous CEST molecules

2.1 Amides (Amide Proton Transfer-APT)

The first molecules that have been imaged through the CEST effect are some endogenous mobile proteins and peptides via saturation of the amide protons in the peptide bonds. In conventional MRI, bound proteins can be easily visualized by magnetization transfer contrast due to their solid-like properties but not mobile proteins and peptides whose protons have relatively long T2 compared to bound proteins. In 2000, the feasibility of imaging mobile proteins was demonstrated with the CEST technique, called Amide Proton Transfer (APT) (Ward et al, 2000). Due to the sensitivity of the CEST signal to pH, this approach was initially developed to monitor pH changes. It has been shown that pH-monitoring through APT allows the detection of cerebral ischemia as pH is reduced during acute ischemia and potentially represents a diagnostic tool in clinical imaging (Zhou et al, 2003b). One of the main concerns in a case of cerebral ischemia is the detection of penumbra, a hypoperfused region affected by ischemia that can be saved through timely therapeutic intervention. In practice, this area is estimated by combining two MRI sequences to estimate the size of the penumbra, a Perfusion Weighted Imaging (PWI) sequence and a Diffusion Weighted Imaging (DWI) sequence. The CEST approach has shown the possibility to distinguish this key region in the treatment of ischemia through pH-weighted imaging (Harston et al, 2015, Sun et al 2007). Since the occurrence of a stroke may be of ischemic or hemorrhagic origin, studies on the distinction of these two events have been carried out. The distinction between cerebral ischemia and intracerebral hemorrhage was emphasized (Jeong et al, 2017, Ma et al, 2017, Wang et al, 2015).

This technique is not only an interesting diagnostic tool for the detection and characterization of cerebral ischemia but also a method to study brain tumors. The use of APT in this case is based on the premise that a brain tumor contains a larger amount of proteins than the surrounding tissue. The feasibility was demonstrated on a gliocarcinoma brain tumor model in rats (Zhou et al 2003a). Compared to other types of clinical acquisition sequences, APT allows a good discrimination of tumors in humans at 3T (Jones et al, 2006, Yang et al 2020). Moreover, it is possible to discriminate high and low-grade tumors (Togao et al, 2014; Wen et al 2010) or high-grade tumors and lymphomas (Jiang et al, 2016). APT was also used to evaluate the treatment of tumors in mice by ultrasound (Hectors et al, 2014). Other distinctions can also be made between malignant and benign tumors and healthy tissue by allying APT and apparent diffusion coefficient ADC (Choi 2018; Law et al, 2018), making this approach an interesting detection tool in clinical practice.

Besides strokes and tumors, APT is also used in models of neurodegenerative diseases. As neurodegenerative diseases such as Alzheimer's and Parkinson's disease are characterized by proteins accumulation and loss of neurons, APT has been used for imaging these pathologies *in vivo*. In Parkinson's disease, different brain areas could be detected according to neuronal loss and protein accumulation (Li et al, 2014; 2017) and for Alzheimer's disease, the aggregation of the protein Tau could be visualized using the APT technique (Wang et al, 2015; Wells et al, 2015). Moreover, APT was used to monitor the effect of a doxycycline-based treatment for Alzheimer’s disease in mouse model of tau pathology (Holmes et al, 2016; Chen et al 2019).

APT is useful for research purposes and also in clinical investigations for diagnosis and to follow-up treatments of several brain pathologies such as ischemia, hemorrhages, tumors

and neurodegenerative diseases as emphasized in the recent review by Zhou et al. 2020. APT could also potentially replace invasive biopsies to provide diagnosis (Sagiyama et al, 2014).

2.2 Glutamate (GluCEST)

Glutamate is the major excitatory neurotransmitter in the brain. It is a key amino acid involved in the control of many functions in the central nervous system such as learning and memory, and is therefore involved in several neurologic diseases like Alzheimer's disease or multiple sclerosis (Kostic et al, 2013; Revett et al, 2013). Excessive concentration can lead to excitotoxicity and neuronal death. Due to its high concentration and its important role in the nervous system, the possibility of glutamate imaging is interesting for the purpose of research on pathophysiology or diagnostic. Glutamate has shown to have a chemical exchange saturation transfer effect named GluCEST (Cai et al, 2012). With this technique, it was demonstrated that middle-cerebral artery occlusion in the rat brain resulted in an increase of GluCEST signal in the ipsilateral region compared with the contralateral region, and intravenous glutamate injection in a model of blood-brain barrier disruption in rat resulted in an elevation of signal in the brain (Cai et al, 2012). This work has also shown the first mapping of glutamate from human brain showing difference between white and gray matter at 7T. Following this work, mapping of glutamate in subcortical regions of the human brain was performed and subcortical regions like amygdala and hippocampus present different contrasts, demonstrating that GluCEST is suitable to reveal anatomical differences of glutamate distribution (Cai et al 2013). GluCEST has been also recently used for clinical purpose to image glutamate after acute traumatic brain injury in human (Mao et al, 2019).

As altered glutamate concentration was reported in the early stages of Alzheimer disease, GluCEST is suitable to image the change in glutamate concentration in the whole brain during the progression of pathology. A glutamate-mapping in the APP-PS transgenic mouse model of Alzheimer's disease has provided a noninvasive biomarker of the disease (Haris et al, 2013a). The use of GluCEST to measure the effect of tau pathology on glutamate levels throughout the brain of a mouse model of tauopathy, showed decreased level of glutamate in the CA sub-region of the hippocampus and in the thalamus (Crescenzi et al, 2014; 2017). The usefulness of this approach was also demonstrated for other pathologies such as Huntington's disease (Pépin et al, 2016; Flament et al, 2018), temporal lobe epilepsy (Davis et al, 2015) and multiple sclerosis (O'Grady et al, 2019).

GluCEST was used to monitor the alteration of glutamate levels in a mouse model of dopamine-deficiency induced by 1-methyl-4-phenyl-1,2,3,6-tetrahydropyridine (MPTP) (Bagga et al, 2016). Other applications could be found by this approach, like the monitoring of the effect of a psychostimulant such as Modafinil, a molecule used in the treatment of narcolepsy and sleep apnea (Haris et al., 2014a) or in a rat model of stress-induced sleep disturbance (Lee et al, 2019c). GluCEST can also be used to monitor the enzymatic activity of a tumor protease that will produce glutamate after cleavage of a specific probe, poly-L-glutamate (PLG) (Haris et al., 2014b).

Using a similar approach for GluCEST, GABA CEST has been recently developed for the detection of GAB in the hippocampus of rat model of preclinical model of epilepsy induced by kainic acid treatment (Lee et al 2019a).

2.3 Glucose (GlucoCEST)

Glucose is the most widely used sugar for metabolism and represents an important energy source for cellular respiration. When entered in cells, glucose is immediately phosphorylated to give glucose-6-phosphate (G6P) and is incorporated in polymer of glycogen and supplies almost all the energy for the brain. The first development of CEST imaging for glucose (GlucoCEST) takes place in 2012 with the detection of D-glucose as a biodegradable MRI agent for cancer detection (Chan et al, 2012). Acid pH environment in the tumor enable the visualization of D-glucose as CEST effect is pH dependent. Injection of D-glucose not only allow the detection of tumor but also showed differences between two different tumor breast cells lines, (MDA-MB-231 and MCF-7) while Positron-emission tomography (PET) and Contrast-Enhanced MRI (CE-MRI) techniques did not. The first use of GlucoCEST for neuroimaging used an injection of 2-deoxy-D-glucose (2DG); this analogue of glucose is not metabolized and is stored in the cells in a phosphorylated form, 2DG-6-phosphate (2DG6P). The level of 2DG gives information on cerebral metabolism, particularly tumors metabolism (Zhang et al, 2014) . This method has been used to monitor the consumption of glucose in the brain and thus to identify active brain regions, since glucose is the major source of energy for the brain (Nasrallah et al, 2013). In their study, Nasrallah *et al.* showed an increase of signal in the cortex and the thalamus, after a 2DG injection, compared with the rest of the brain. 3-O-methyl-D-glucose, another analogue of glucose was recently used to detect accumulation of glucose in in rodent model of brain tumor (Sehgal et al, 2019) and the brain of healthy human and brain tumor patients (Xu et al, 2019). Central level of endogenous glucose monitored with GlucoCEST MRI is a good indicator of neuronal activation since the same brain areas are also activated with BOLD fMRI as shown in rats (Roussel et al, 2019).

GlucoCEST can be also used to study the dynamic perfusion of a cerebral tumor (Xu et al 2015). This study explored the integrity of the Blood-Brain Barrier (BBB) and the authors tested the feasibility of performing Dynamic Glucose Enhanced (DGE) imaging. They showed an increase of the signal during and after injection of D-glucose in the tumor compared to other cerebral tissue. In addition, Wang et al, using DGE and comparing it to PET showed a good correlation between these two techniques in patients with head and neck cancer (Wang et al, 2016). This approach could avoid excessive ionization of patients by substituting PET with DGE in some cases. The novelty of these approaches is to be able to produce biodegradable markers like D-glucose and 2DG, approved by the Food and Drug Administration (FDA) to boost the signal. The disadvantage of GlucoCEST is to require an injection of non-metabolized glucose analogs to visualize the signal because natural glucose is quickly incorporated and metabolized.

2.4 Myo-Inositol (MICEST)

Among endogenous molecules, Myo-Inositol has also a CEST signal (MICEST). Myo-inositol is a carbocyclic sugar found in large quantity in the brain. It is one of the metabolites usually visible with MRS and playing an important role in cells as precursor of secondary messenger in eukaryotic cells in the form of inositol phosphate, phosphatidylinositol and phosphatidylinositol phosphate which are also constituents of the lipid membranes of the cells as well as myelin in the central nervous system (Fisher et al, 2002). Altered concentrations of myo-inositol have been detected in many brain disorders like Alzheimer's disease, multiple sclerosis and brain tumors. Myo-inositol has been first studied by MRS and in 2011, the idea of applying the CEST effect to visualize myo-inositol was carried out, in order to have a better spatial resolution of myo-inositol distribution. A brain mapping of myo-

inositol on healthy human volunteers showed significantly higher MICEST signal in white matter than in gray matter at 7T (Haris et al, 2011). MICEST was subsequently used for the study of myo-inositol concentrations in mice model of Alzheimer's disease (APP-PS1). The APP-PS1 mice showed a higher MICEST contrast than wild-type control with concomitant increase in myo-inositol concentration as measured through proton spectroscopy (Haris et al, 2013b). High resolution mapping of myo-inositol with MICEST is a useful technique for monitoring the regional changes of myo-inositol at different disease states. Contrary to glucose, MICEST does not require any exogenous contrast administration and due to its non-invasive nature, mapping of myo-inositol provides a new disease biomarker.

2.5 Creatine (CrCEST)

Creatine is a metabolite derived from amino acid (glycine, arginine and methionine) and present mainly in the muscle fibers and to a lesser extent in the brain. In cells, creatine helps to supply energy, particularly in muscles. Enzymes called creatine kinases, forming phosphocreatine used to recycle adenosine triphosphate (ATP), phosphorylate a part of the creatine incorporated into the cells. This phosphocreatine can provide a phosphate group to ADP making ATP which is a major source of cellular energy and vice versa (Joncquel-Chevalier Curt et al, 2015). Creatine was first detected by MRS and in 2012, a high-resolution imaging of creatine was developed using the CEST technique (CrCEST), allowing a better spatial resolution imaging without a signal contamination from phosphocreatine (Haris et al, 2012). CrCEST provided a new method to measure the changes in creatine *in vivo* in various pathological conditions. The first use of CrCEST was done on the muscle to map the energetic changes of the muscle during exercises, with a high spatial resolution (Kogan et al, 2014). CEST imaging applied to creatine has also been used in the field of neuroimaging by studying the distribution of creatine in cerebral tumors (Cai et al, 2015). CrCEST signal is interesting for the detection of creatine, a bioenergetics marker of tumor metabolism. This signal could be used to determine the tumor grade and to monitor the effect of treatments (Cai et al, 2017). CrCEST was also used to study epileptic seizures. A first study showed that following an epileptic seizure induced in mice, an increase in creatine signal is observed in the affected area (Lee et al, 2019b). This technique would permit to follow sudden metabolic changes over time.

3 Exogenous CEST molecules

There are mainly three categories of CEST exogenous contrast agents. 1) Diamagnetic agents, or DiaCEST agents, have exchangeable protons in their chemical structure most of the time belonging to amine (–NH), acid or alcohol (–OH) functions. Their ^{1}H NMR resonance signal appears around 5 ppm compared to the free water signal. Observation of this chemical shift requires a relatively slow exchange constant, which limits the observed effect compared to the dose injected. 2) Paramagnetic agents, or ParaCEST agents, are complexes of paramagnetic ions, most often of rare earths, which transiently bind protons whose chemical shifts of the protons are much greater, possibly exceeding hundreds of ppm. 3) Liposome agents or LipoCEST which is a special case of ParaCEST agents and which consists in using liposomes encapsulating a paramagnetic lanthanide complex as contrast.

3.1 Exogenous diamagnetic agents (DiaCEST)

The first CEST agents studied are diamagnetic molecules comprising exchangeable protons via acid-base properties in the Brönsted sense, therefore sensitive to the pH of the environment and/or to temperature variations (Ward et al., 2000). They bring together either small synthetic organic molecules, more rarely polymers, or compounds of biological origin. Most diamagnetic compounds exhibit a resonance frequency of their labile proton (s) that does not differ by more than 5 ppm (or 315 Hz at 1.5T) from the frequency of free water in the surrounding medium, limiting the efficiency of selective irradiation of exchangeable protons (Zhang et al., 2001). In addition, the *in vivo* use of diamagnetic compounds may be compromised by the lack of discrimination with the effect of endogenous CEST agents, which often have a very large signal. Despite these drawbacks, the harmlessness of diamagnetic compounds remains interesting and it is possible to use them either as an intrinsic signal from the tissues or to account for certain metabolic processes or environmental factors (pH, temperature) or even to reveal the presence of other substances by activating their contrast after specific interaction (Chahid et al, 2014).

In the 2000's, exogenous diamagnetic molecules were studied as potential CEST contrast agents. They are compounds, having diamagnetic properties like endogenous molecules and a proton exchange site permitting the detection by CEST. They were developed as a substitute for metal-based contrast agent, like gadolinium complexes, due to the toxicity of these metal ions at high doses and once administered, the contrast persists until the organism eliminates it. Exogenous contrast agents possessing specific chemical groups which could have CEST properties permitting a "switch on/off" of the signal under physiological conditions have been developed (Ward et al, 2000). Several diamagnetic molecules with CEST properties have been found such as salicylic acid and its analogues (Yang et al, 2013) or anthranilic acid analogs (Song et al, 2015). These diamagnetic agents were quickly used in the field of nanotechnology. They boosted a relatively low CEST signal by increasing locally the concentration of contrast agents in a vector (Zhao et al, 2008). Citicoline, a diamagnetic molecule, possessing also neuroprotective properties and used to treat cerebral injuries and diseases, has shown promising results (Liu et al, 2016). In a cerebral ischemia model in the rat, these citicoline-liposomes targeted against Vascular Cell Adhesion Molecule (VCAM)-1 can accumulate in the damaged area of the brain and improve drug delivery. Liposomes containing citicoline represents a theranostic system, where the therapeutic agent can be detected directly by CEST MRI.

Small proteins like Lysine-rich protein (LRP) have diaCEST properties and are sensitive to pH variations. The labile protons of the lysine units of the LRP are exchangeable in the intracellular basic medium that induce a local acidification of the tissue. In a recent study, LRP have been used to detect a glioma in a murine model with quite high sensitivity since a decrease of one pH unit induces a ten fold reduction of the CEST signal intensity (Perlman et al, 2020).

Recently a new category of diaCEST molecule were developed using carbon dots (C-dots) (Zhang et al, 2019). C-dots are quasi-spherical carbogenic nanoparticles of several nm in size, they constitute a new type of organic materials composed primarily of carbon, oxygen, and hydrogen, they are considered to be more biocompatible than the heavy metal-based quantum dots. Arginine-modified C-dots encapsulated in liposome were successfully used to label human U-87 MG glioma cells that can be therefore detected after injection in the striatum of mice (Zhang et al, 2019). This preclinical data obtained with this novel diaCEST agent are promising for future brain exploration and clinical investigation using grafted cell therapy.

Moreover, contrast agents having properties in other imaging techniques have been obtained, combining a molecule having a CEST effect with other molecules having properties for optical imaging, like rhodamine (Liu et al, 2012).

3.2 Exogenous paramagnetic agents (ParaCEST)

ParaCEST contrast agents combine paramagnetic properties, linked to the presence in their chemical structure of a certain number of unpaired electrons possessing a large electronic spin magnetic moment, and the ability to exchange one or more water molecules of hydration with the surrounding aqueous medium. The particular advantage is the significant chemical shift of the protons in water induced by the contrast agent which allows a much more selective CEST effect than that obtained with DiaCEST agents. In addition, the ability to change the structure and add exchange sites can optimize their detection at low concentrations (Aime et al, 2002; Zhang et al 2003). Like diamagnetic contrast agents, *in vivo* visualization is difficult because the magnetization transfer from endogenous macromolecules reduces the CEST sensitivity. To improve their sensitivity, the paraCEST agents have been incorporated to nanocarriers like dendrimers, adenovirus particles and perfluorocarbon nanoparticles (Li et al, 2011). The first dendrimer paraCEST agents were prepared through coupling Yb3+-DOTAM complexes to a poly(propylene imine) dendrimer to obtain a pH-sensitive CEST contrast at Δ = -15 ppm (Pikkemaat et al 2007). The small size (~7–12 nm) of dendrimers have the advantage over the other particles, because its smaller size can possibly improve tissue penetration and the inclusion of tumor specific drug release mechanisms.

ParaCEST contrast agents are used for molecular imaging in various fields including neuroimaging. First promising works concerns the development of calcium-sensitive ParaCEST contrast agent. Calcium or magnesium binding to the lanthanide complexes reduce the exchange of the amide protons inducing a decrease of the CEST effect. This kind of contrast agents represent an interesting tool for monitoring neuronal activity (Angelovski et al, 2011).

Nano-sized paraCEST imaging contrast agent using a dual-modality agent were developed for detecting gliomas at MRI and microscopic scales. The ParaCEST MRI contrast agent such as Eu-DOTA-Gly4 or a clinical relevant Gd-DOTA and fluorescent molecules Dylight680 were conjugated on the surface of a G5 polyamidoamine dendrimer to create a dual mode MRI-optical imaging nanoparticle and used for the detection of a U87 glioma model in mouse with a 3T scanner (Ali et al, 2012, Gonawala and Ali 2017). The sophistication of these structures appears to create a new class of contrast agents called multi-modal in which paraCEST molecules have found their place.

3.3 Exogenous liposome agents (LipoCEST)

Silvio Aime and his collaborators (2005) are pioneers in the field of LipoCEST and introduced the first proof of concept of this new family of contrast agents, (Aime et al, 2005). The LipoCEST approach was developed by encapsulating the contrast agent in a liposome (Chan et al, 2014a). Liposomes are closed vesicles, most often submicron, delimited by one or more bilayers of lipids enclosing a fraction of the aqueous medium in which they were formed. Their structure is similar to the cell membrane which makes liposomes the ideal

models for studying biological processes. Their lipid composition can be modulated to cross natural barriers (like blood brain barrier), and to control the release of their content (according to temperature or pH).

In LipoCEST agent, the liposome structure makes possible the differentiation of the two groups of water molecules necessary to obtain a CEST effect by regulating the rate of water exchange between the internal and external compartment of the liposome. The high sensitivity expected for a LipoCEST agent comes from the fact that all the water molecules contained in the internal volume of the liposomes will contribute to the transfer of magnetization, which is considerable in comparison with molecular ParaCEST agents that bind only one or two water molecules per unit. Optimized LipoCEST agent using 200 nm diameter liposome with a polyethylene glycol chains coated surface to ensure their future stability in the blood compartment were developed for in vivo imaging. The properties of the systems were evaluated both in relation to the vesicular structure and in relation to the magnetic response (Chahid 2012).

Flament et al. prepared a specific lipoCEST agent by conjugation of Tm(III)-complexes to RGD tripeptide to target integrin α(v)β(3) receptors that are involved in tumour angiogenesis. After intravenous injection, this lipoCEST agent allowed the detection of brain tumor induced by intracerebral injection of U87MG cells in mice imaged at 7T, and specifity of the staining were confirmed by immunohistochemical colocalisation of RGD-lipoCEST with the $\alpha_v\beta_3$ receptors in the tumor region (Flament et al, 2013).

More recently, an injectable liposomal hydrogel (LipoCEST MRI) was developed to monitor *in vivo* treatment using a 3T clinical field (Han et al 2020). In this study, the liposomal hydrogel is loaded with barbiturique acid an injected in the brain of mice. The animals were imaged 4 h, 1, and 3 d after injection at 3.0 T. The results showed that CEST contrast at -3.4 ppm provided an estimated number of liposomes and CEST contrast at 5 ppm provided an estimated amount of encapsulated drug. CEST contrast at 5 ppm decreased by 1.57%, while the contrast at -3.4 ppm remained constant over the 3 days *in vivo*, demonstrating different release kinetics of these components from the hydrogel (Han et al 2020).

These studies demonstrated the promising role of lipoCEST as contrast agent for the observation of brain tissue but also as new tools for monitoring drug delivery for the treatment of brain tumour.

4 Advantage and drawback of CEST technique

One of the main advantage of the CEST contrast agents for MRI is to give neurochemical information with a high spatial resolution that is of a particular importance according to the complex brain anatomy. Compared to MRS, CEST contrast agents present a similar sensitivity as observed for glutamate detection with GluCEST (Cai et al, 2013), but MRS is limited to low spatial resolution. Compared to PET, GluCEST give similar distribution of glutamate in white and grey matter as demonstrated in human mapping of the metabotropic glutamate receptor subtype 5 (Ametamey et al, 2007). Similar observations were made for the detection of 2-Deoxy-D-Glucose uptake in a mice model of Alzheimer disease using glucoCEST and 18 FDG-PET, with a better image resolution for glucoCEST (Tolomeo et al, 2018). The advantages of both techniques are now available with clinical and pre-clinical combined PET-MR system.

The specificity of CEST agent to detect specific molecule is similar to that observed using MRS. However, this specificity should be also carefully checked since CEST effect of two

molecules may overlapped when the molecules present close exchangeable protons. CEST effect of one molecule can contribute to the CEST effect of another expected molecule. Cai et al (2012) identified a small contribution of GABA and creatinine to the CEST effect of GluCEST, due to the $–NH_2$ protons. Similarly, the detection of glycogen by GlycoCEST is modified by the GlucoCEST effect of glucose at equivalent concentration because glucose has more exchangeable protons than glycogen (Van Zijl et al, 2007). The overlapping of CEST effects of different molecules is affected by the radiofrequency B1 as shown for MiCEST detection of myo-inositol (Haris et al, 2011), a parameter that may be used to improve the specificity of the detection.

Compared to molecular imaging like TEP, CEST effect induced by endogenous molecules is non-invasive which is important for in vivo and clinical studies, an advantage that disappeared with paraCEST and DiaCEST molecules that should be injected. These later compounds have to cross the BBB to reach the brain in a way that will not modify neuronal physiology. Glucose analogues like 2DG or 3 O-methyl glucose cross the BBB with the glucose transporter 1 localized on endothelial cellular membrane. For other compounds, BBB can be osmotically open using hypertonic mannitol solutions as previously described by Kroll and Neuwelt (Kroll and Neuwelt, 1998), or using ultrasound transcranial stimulation in combination with gas-filled microbubbles as previously used for manganese enhanced MRI (Howles et al, 2010).

Magnitude of CEST effect appears to be better at higher magnetic field strength as shown for glycoCEST (Van Zijl et al, 2007), being higher at 9.4 than at 4.7T. The same observation was made for gluCEST, the effect being higher at 9.4T in rodents than at 7T in human brains (Cai et al, 2012). According to these studies, it appears that the CEST compounds should be used at high magnetic fields and that they would be less powerful, with a lower sensitivity with standard scanner at 3T.

Conclusion

CEST technique has proved to be an innovative tool in the field of molecular imaging in MRI. Compared to other MRI contrast agents like gadolinium- and iron-based contrast agents, which modify the relaxivity of the surrounding tissues, CEST signal is activated only by a specific radiofrequency wave permitting an on/off switch signal, and a noise free signal. Such properties should make possible dual labelling with distinct CEST agents. The stability of these paramagnetic agents has to be improved regarding to their sensitivity to temperature, which could be modified under RF stimulation. Their ability to give a strong signal under physiological conditions and at low concentrations is also a weakness of these agents. The strength of the signal is linked to the number exchangeable proton (OH, NH, NH2 moieties) and CEST effect will be increase by increasing the number of exchanging groups by grafting them on specific agents. This approach is particularly promising for lipoCEST. It is therefore possible to shape CEST agent for specific targets.

CEST technique is a wide field of broad research with a real potential development in the field of molecular of neuroimaging. Applications of CEST imaging in human using endogenous molecules are attractive because nothing is injected and therefore do not require any administrative approval (like FDA or CE for example). In addition, imaging endogenous molecule (glucose, glutamate…) overcomes the problem of crossing the BBB. These CEST imaging methods are useful in the study of neurodegenerative diseases, tumors and strokes

as well as for psychiatric research (recent review by Shaffer et al, 2020). The first clinical application have been already done as shown on the Figure 2 (Goerke et al, 2019). They make MRI the gold standard for the detection of neurotransmission disorders or tumor boundary delimitation in addition to MRS.

Acknowledgement
The authors wish to thank Dr Eva Jakab Thot (CBM CNRS UPR 4301, Orléans France) for reviewing and advices for the preparation of the manuscript. K. El Mamoune was granted by Siemens Healthcare SAS, Saint Denis, France, and Association Nationale Recherche Technologie (ANRT, Grant n° 1250/2015).

References

Aime S. Barge A., Delli Castelli D., Fedeli F., Mortillaro A., Nielsen F.U., Terreno E., 2002. Paramagnetic Lanthanide(III) complexes as pH-sensitive chemical exchange saturation transfer (CEST) contrast agents for MRI applications. Magn. Reson. Med. 47(4): 639-648.

Aime S., Delli Castelli D., Terreno E., 2005. Highly Sensitive MRI Chemical Exchange Saturation Transfer Agents Using Liposomes. Angew. Chem. Int. Ed. 44: 5513–5515. Doi.org/10.1002/anie.200501473

Ali M.M, Pi Bhuiyan M., Janic B., Varma N. Rs, Mikkelsen T., Ewing J.R., Knight R. A., Pagel M. D., Arbab A.S., 2012. A nano-sized PARACEST-fluorescence imaging contrast agent facilitates and validates in vivo CEST MRI detection of glioma. Nanomedicine (Lond). 7(12): 1827-37. Doi: 10.2217/nnm.12.92. Epub 2012 Aug 14

Ametamey S.M., Treyer V., Streffer J., Wyss M.T., Schmidt M., Blagoev M., Hintermann S., Auberson Y., Gasparini F., Fischer U.C., Buck A., 2007. Human PET studies of metabotropic glutamate receptor subtype 5 with 11C-ABP688. J Nucl Med. 48(2):247-52. PMID: 17268022.

Angelovski G., Chauvin T., Pohmann R., Logothetis N. K. and Tóth É., 2011. Calcium-responsive paramagnetic CEST agents. Bioorg. Med. Chem. 19(3): 1097-1105.

Bagga P., Crescenzi R., Krishnamoorthy G., Verma G., Nanga R.P., Reddy D., Greenberg J., Detre J.A., Hariharan H., Reddy R., 2016. Mapping the alterations in glutamate with GluCEST MRI in a mouse model of dopamine deficiency. J Neurochem. 139(3):432-439. doi: 10.1111/jnc.13771

Cai K., Haris M., Singh A., Kogan F., Greenberg J.H., Hariharan H., Detre J.A., Reddy R., 2012. Magnetic resonance imaging of glutamate. Nat Med. 18(2):302-6. doi: 10.1038/nm.2615.

Cai K., Singh A., Poptani H., Li W., Yang S., Lu Y., Hariharan H., Zhou X.J., Reddy R., 2015. CEST signal at 2ppm (CEST@2ppm) from Z-spectral fitting correlates with creatine distribution in brain tumor. NMR Biomed. 28(1):1-8. doi: 10.1002/nbm.3216

Cai K., Singh A., Roalf D.R., Nanga R.P., Haris M., Hariharan H., Gur R., Reddy R., 2013. Mapping glutamate in subcortical brain structures using high-resolution GluCEST MRI. NMR Biomed. 26(10):1278-1284. doi: 10.1002/nbm.2949

Cai K., Tain R.W., Zhou X.J., Damen F.C., Scotti A.M., Hariharan H., Poptani H., Reddy R., 2017. Creatine CEST MRI for Differentiating Gliomas with Different Degrees of Aggressiveness. Mol Imaging Biol. 19(2):225-232. doi: 10.1007/s11307-016-0995-0.

Chahid B., 2012. Développement et caractérisation de nouveaux agents de contraste lipidiques ultrasen-sibles pour l'imagerie par résonnance magnétique destinés à l'imagerie moléculaire. Université Paris Sud - Paris XI. https://tel.archives-ouvertes.fr/tel-01124083/document

Chahid B., Vander Elst L., Flament J., Boumezbeur F., Medina C., Por M., Muller R. N., Lesieur S., 2014. Entrapment of a neutral Tm(III)-based complex with two inner-sphere coordinated water molecules into PEG-stabilized vesicles: towards an alternative strategy to develop high-performance LipoCEST contrast agents for MR imaging. Contrast Media Mol Imaging. 9(6):391-9. Doi: 10.1002/cmmi.1589

Chan K.W., McMahon M.T., Kato Y., Liu G., Bulte J.W., Bhujwalla Z.M., Artemov D., van Zijl P.C., 2012. Natural D-glucose as a biodegradable MRI contrast agent for detecting cancer. Magn Reson Med. 68(6):1764-73. doi: 10.1002/mrm.24520.

Chan K. W. Y., Bulte J. W. M. and McMahon M. T., 2014a. Diamagnetic chemical exchange saturation transfer (diaCEST) liposomes: physicochemical properties and imaging applications: diaCEST liposomes. Wiley Interdiscip. Rev. Nanomed. Nanobiotechnol. 6(1): 111-124.

Chan K.W., Yu T., Qiao Y., Liu Q., Yang M., Patel H., Liu G., Kinzler K.W., Vogelstein B., Bulte J.W., van Zijl P.C., Hanes J., Zhou S., McMahon M.T., 2014b. A diaCEST MRI approach for monitoring liposomal accumulation in tumors. J. Controlled Release 180: 51-59.

Chen L., Wei Z., Chan K.W.Y., Cai S., Liu G., Lu H., Wong P.C., van Zijl P.C.M., Li T. and Xu J., 2019. Protein aggregation linked to Alzheimer's disease revealed by saturation transfer MRI. Neuroimage. 188:380-390. doi: 10.1016/j.neuroimage.2018.12.018.

Choi S. H., 2018. Can Amide Proton Transfer MRI Distinguish Benign and Malignant Head and Neck Tumors? Radiology, 288(3): 791-792. doi: 10.1148/radiol.2018180914.

Crescenzi R., De Brosse C., Nanga R.P., Reddy S., Haris M., Hariharan H., Iba M., Lee V.M., Detre J.A., Borthakur A., Reddy R., 2014. In vivo measurement of glutamate loss is

associated with synapse loss in a mouse model of tauopathy. Neuroimage. 101:185-192. doi: 10.1016/j.neuroimage.2014.06.067.

Crescenzi R., DeBrosse C., Nanga R.P., Byrne M.D., Krishnamoorthy G., D'Aquilla K., Nath H., Morales K.H., Iba M., Hariharan H., Lee V.M., Detre J.A., Reddy R., 2017. Longitudinal imaging reveals subhippocampal dynamics in glutamate levels associated with histopathologic events in a mouse model of tauopathy and healthy mice. Hippocampus. 27(3):285-302. doi: 10.1002/hipo.22693.

Davis K.A., Nanga R.P., Das S., Chen S.H., Hadar P.N., Pollard J.R., Lucas T.H., Shinohara R.T., Litt B., Hariharan H., Elliott M.A., Detre J.A., Reddy R., 2015. Glutamate imaging (GluCEST) lateralizes epileptic foci in nonlesional temporal lobe epilepsy. Sci Transl Med. 7(309):309ra161. doi: 10.1126/scitranslmed.aaa7095.

Fisher S. K., Novak J. E. and Agranoff B. W., 2002. Inositol and higher inositol phosphates in neural tissues: homeostasis, metabolism and functional significance: Inositol and inositol polyphosphates in CNS. J. Neurochem., 82(4):736-754.

Flament J., Geffroy F., Medina C., Robic C., Mayer J.F., Mériaux S., Valette J., Robert P., Port M., Le Bihan D., Lethimonnier F., Boumezbeur F., 2013. In vivo CEST MR imaging of U87 mice brain tumor angiogenesis using targeted LipoCEST contrast agent at 7 T.Magn Reson Med. 69(1):179-87. doi: 10.1002/mrm.24217.

Flament J., Hantraye P., and Valette J., 2018. In Vivo Multidimensional Brain Imaging in Huntington's Disease Animal Models », in Huntington's Disease, vol. 1780. S. V. Precious, A. E. Rosser, et S. B. Dunnett, Éd. New York, NY: Springer New York, p. 285-301.

Goerke S., Soehngen Y., Deshmane A., Zaiss M., Breitling J., Boyd P.S., Herz K., Zimmermann F., Klika K.D., Schlemmer H.P., Paech D., Ladd M.E. and Bachert P., 2019. Relaxation-compensated APT and rNOE CEST-MRI of human brain tumors at 3 T. Magn Reson Med. 82(2):622-632. doi: 10.1002/mrm.27751.

Gonawala S. and Ali M.M., 2017. Application of Dendrimer-based Nanoparticles in Glioma Imaging. J Nanomed Nanotechnol. 8: 444. Doi: 10.4172/2157-7439.1000444

Grover V. P. B., Tognarelli J. M., Crossey M. M. E., Cox I. J., Taylor-Robinson S. D., and McPhail M. J. W., 2015. Magnetic Resonance Imaging: Principles and Techniques: Lessons for Clinicians. J. Clin. Exp. Hepatol. 5(3): 246-255.

Han X., Huang J., To A. K. W., Lai J. H. C., Xiao P., Wu E. X., Xu J., Chan K.W.Y., 2020. CEST MRI detectable liposomal hydrogels for multiparametric monitoring in the brain at 3T. Theranostics. 10(5):2215-2228. Doi: 10.7150/thno.40146

Haris M., Cai K., Singh A., Hariharan H. and Reddy R., 2011. In vivo mapping of brain myo-inositol. NeuroImage, 54(3): 2079-2085. doi: 10.1016/j.neuroimage.2010.10.017

Haris M., Nanga R.P., Singh A., Cai K., Kogan F., Hariharan H., Reddy R., 2012. Exchange rates of creatine kinase metabolites: feasibility of imaging creatine by chemical exchange saturation transfer MRI. NMR Biomed. 25(11):1305-9. doi: 10.1002/nbm.2792.

Haris M., Nath K., Cai K., Singh A., Crescenzi R., Kogan F., Verma G., Reddy S., Hariharan H., Melhem E.R., Reddy R., 2013a. Imaging of glutamate neurotransmitter alterations in Alzheimer's disease. NMR Biomed. 26(4):386-391. doi: 10.1002/nbm.2875.

Haris M., Singh A., Cai K., Nath K., Crescenzi R., Kogan F., Hariharan H., Reddy R., 2013b. MICEST: A potential tool for non-invasive detection of molecular changes in Alzheimer's disease. J. Neurosci. Methods. 212(1): 87-93. doi: 10.1016/j.jneumeth.2012.09.025

Haris M., Singh A., Cai K., Nath K., Verma G., Nanga RP., Hariharan H., Detre JA., Epperson N., Reddy R., 2014a. High resolution mapping of modafinil induced changes in glutamate level in rat brain. PLoS One. 9(7):e103154. doi: 10.1371/journal.pone.0103154.

Haris M., Singh A., Mohammed I., Ittyerah R., Nath K., Nanga RP5. Debrosse C., Kogan F., Cai K, Poptani H., Reddy D., Hariharan H. and Reddy R., 2014b. In vivo magnetic resonance imaging of tumor protease activity. Sci Rep. 4:6081. doi: 10.1038/srep06081.

Harston G.W., Tee Y.K., Blockley N., Okell T.W., Thandeswaran S., Shaya G., Sheerin F., Cellerini M., Payne S., Jezzard P., Chappell M., Kennedy J., 2015. Identifying the ischaemic penumbra using pH-weighted magnetic resonance imaging. Brain. 138(Pt 1):36-42. doi: 10.1093/brain/awu374.

Hectors S. J. C. G., Jacobs I., Strijkers G. J., and Nicolay K., 2014. Amide proton transfer imaging of high intensity focused ultrasound-treated tumor tissue: APT Imaging of HIFU-Treated Tumor Tissue. Magn. Reson. Med. 72(4): 1113-1122.

Holmes H.E., Colgan N., Ismail O., Ma D., Powell N.M., O'Callaghan J.M., Harrison I.F., Johnson R.A., Murray T.K., Ahmed Z., Heggenes M., Fisher A., Cardoso M.J., Modat M., Walker-Samuel S., Fisher E.M., Ourselin S., O'Neill M.J., Wells J.A., Collins E.C., Lythgoe M.F., 2016. Imaging the accumulation and suppression of tau pathology using multiparametric MRI. Neurobiol Aging. 39:184-94. doi: 10.1016/j.neurobiolaging.2015.12.001

Howles G.P., Qi Y., Johnson G.A., 2010. Ultrasonic disruption of the blood-brain barrier enables in vivo functional mapping of the mouse barrel field cortex with manganese-enhanced MRI. Neuroimage 50(4):1464-71. doi: 10.1016/j.neuroimage.2010.01.050

Jeong H-K., Han K., Zhou J., Zhao Y., Choi U.S., Lee S-K and Ahn S.S., 2017. Characterizing Amide Proton Transfer Imaging in Haemorrhage Brain Lesions Using 3T MRI. Eur Radiol. 27(4):1577-1584. doi: 10.1007/s00330-016-4477-1.

Jiang S., Yu H., Wang X., Lu S., Li Y., Feng L., Zhang Y., Heo H.Y., Lee D.H., Zhou J., Wen Z., 2016. Molecular MRI differentiation between primary central nervous system lymphomas

and high-grade gliomas using endogenous protein-based amide proton transfer MR imaging at 3 Tesla. Eur Radiol. 26(1):64-71. doi: 10.1007/s00330-015-3805-1

Joncquel-Chevalier Curt M., Voicu P.M., Fontaine M., Dessein A.F., Porchet N., Mention-Mulliez K., Dobbelaere D., Soto-Ares G., Cheillan D., Vamecq J., 2015. Creatine biosynthesis and transport in health and disease. Biochimie 119:146-165. doi: 10.1016/j.biochi.2015.10.022.

Jones C. K., Schlosser M. J., van Zijl P. C. M., Pomper M. G., Golay X., and Zhou J., 2006. Amide proton transfer imaging of human brain tumors at 3T. Magn. Reson. Med. 56(3): 585-592.

Kim M., Gillen J., Landman B.A., Zhou J., Van Zijl P.C.M., 2009. Water saturation shift referencing (WASSR) for chemical exchange saturation transfer (CEST) experiments. Magn. Reson. Med. 61(6):1441–50. doi: 10.1002/mrm.21873

Kogan F., Haris M., Debrosse C., Singh A., Nanga R.P., Cai K., Hariharan H., Reddy R., 2014. In vivo chemical exchange saturation transfer imaging of creatine (CrCEST) in skeletal muscle at 3T. J Magn Reson Imaging. 40(3):596-602. doi: 10.1002/jmri.24412.

Kostic M., Zivkovic N., and Stojanovic I., 2013. Multiple sclerosis and glutamate excitotoxicity. Rev Neurosci. 24(1):71-88. doi: 10.1515/revneuro-2012-0062.

Kroll R. A. and Neuwelt E. A., 1998. Outwitting the blood-brain barrier for therapeutic purposes: osmotic opening and other means. Neurosurgery 42(5):1083-99. doi: 10.1097/00006123-199805000-00082

Law B.K.H., King A.D., Ai Q.Y., Poon D.M.C., Chen W., Bhatia K.S., Ahuja A.T., Ma B.B., Ka-Wai Yeung D., Fai Mo F.K., Wang Y.X., Yuan J., 2018. Head and Neck Tumors: Amide Proton Transfer MRI. Radiology. 288(3):782-790. doi: 10.1148/radiol.2018171528

Lee D.H., Lee D.W., Kwon J.I., Kim S.T., Woo C.W., Kon Kim J., Won Kim K., Seong Lee J., Gon Choi C., Suh .JY., Choi Y. and Woo D.C., 2019a. Changes to gamma-aminobutyric acid levels during short-term epileptiform activity in a kainic acid-induced rat model of status epilepticus: A chemical exchange saturation transfer imaging study. Brain Res. 1717:176-181. doi: 10.1016/j.brainres.2019.04.010).

Lee D.H., Lee D.W., Kwon J.I., Woo C.W., Kim S.T., Lee J.S., Choi C.G., Kim K.W., Kim J.K., Woo D.C., 2019b. In Vivo Mapping and Quantification of Creatine Using Chemical Exchange Saturation Transfer Imaging in Rat Models of Epileptic Seizure. Mol Imaging Biol. 21(2):232-239. doi: 10.1007/s11307-018-1243-6.

Lee D.H., Woo C.W., Kwon J.I., Chae Y.J., Ham S.J., Suh J.Y., Kim S.T., Kim J.K., Kim K.W., Woo D.C., Lee D.W., 2019c. Cerebral mapping of glutamate using chemical exchange saturation

transfer imaging in a rat model of stress-induced sleep disturbance at 7.0T. J Magn Reson Imaging. 50(6):1866-1872. doi: 10.1002/jmri.26769.

Li A.X., Suchy M., Li C., Gati J.S., Meakin S., Hudson R.H., Menon R.S., Bartha R., 2011. In vivo detection of MRI-PARACEST agents in mouse brain tumors at 9.4 T. Magn Reson Med. 66(1):67-72. doi: 10.1002/mrm.22772

Li C., Peng S., Wang R., Chen H., Su W., Zhao X., Zhou J., Chen M., 2014. Chemical exchange saturation transfer MR imaging of Parkinson's disease at 3 Tesla. Eur Radiol. 24(10):2631-9. doi: 10.1007/s00330-014-3241-7

Li C., Chen M., Zhao X., Wang R., Chen H., Su W., Li S., Lou B., Song G., Zhang S., Zhang J., Zhou J., 2017. Chemical Exchange Saturation Transfer MRI Signal Loss of the Substantia Nigra as an Imaging Biomarker to Evaluate the Diagnosis and Severity of Parkinson's Disease. Front Neurosci. 11:489. doi: 10.3389/fnins.2017.00489.

Liu G., Moake M., Har-el Y.E., Long C.M., Chan K.W., Cardona A., Jamil M., Walczak P., Gilad A.A., Sgouros G., van Zijl P.C., Bulte J.W., McMahon M.T., 2012. In vivo multicolor molecular MR imaging using diamagnetic chemical exchange saturation transfer liposomes. Magn Reson Med. 67(4):1106-1113. doi: 10.1002/mrm.23100

Liu G., Song X., Chan K.W., McMahon M.T., 2013. Nuts and bolts of chemical exchange saturation transfer MRI. NMR Biomed. 26(7):810-828. doi: 10.1002/nbm.2899

Liu H., Jablonska A., Li Y., Cao S., Liu D., Chen H., Van Zijl P.C., Bulte J.W.M., Janowski M., Walczak P., Liu G., 2016. Label-free CEST MRI Detection of Citicoline-Liposome Drug Delivery in Ischemic Stroke. Theranostics, 6(10): 1588-1600.doi: 10.7150/thno.15492.

Ma X., Bai Y., Lin Y., Hong X., Liu T., Ma L., Haacke E.M., Zhou J., Wang J., Wang M., 2017. Amide proton transfer magnetic resonance imaging in detecting intracranial hemorrhage at different stages: a comparative study with susceptibility weighted imaging. Sci Rep. 7:45696. doi: 10.1038/srep45696.

Mao Y., Zhuang Z., Chen Y., Zhang X., Shen Y., Lin G., Wu R., 2019. Imaging of glutamate in acute traumatic brain injury using chemical exchange saturation transfer. Quant Imaging Med Surg. 9(10):1652-1663. doi: 10.21037/qims.2019.09.08.

Nasrallah F. A., Pagès G., Kuchel P. W., Golay X. and Chuang K.-H., 2013. Imaging brain deoxyglucose uptake and metabolism by glucoCEST MRI. J. Cereb. Blood Flow Metab. 33(8): 1270-1278.

O'Grady K.P., Dula A.N., Lyttle B.D., Thompson L.M., Conrad B.N., Box B.A., McKeithan L.J., Pawate S., Bagnato F., Landman B.A., Newhouse P., Smith S.A., 2019. Glutamate-sensitive imaging and evaluation of cognitive impairment in multiple sclerosis. Mult Scler. 25(12):1580-1592. doi: 10.1177/1352458518799583

Pépin J., Francelle L., Carrillo-de Sauvage M.A., de Longprez L., Gipchtein P., Cambon K., Valette J., Brouillet E., Flament J., 2016. In vivo imaging of brain glutamate defects in a knock-in mouse model of Huntington's disease. Neuroimage. 139:53-64. doi: 10.1016/j.neuroimage.2016.06.023.

Perlman O., Ito H., Gilad A. A., McMahon M.T., Chiocca E.A., Nakashima H., Farrar C.T., 2020. Redesigned Reporter Gene for Improved Proton Exchange-based Molecular MRI Contrast, Scientific Reports, 10: 20664. Doi: 10.1038/s41598-020-77576-z

Pikkemaat J.A., Wegh R.T., Lamerichs R., van de Molengraaf R.A., Langereis S., Burdinski D., Raymond A.Y.F., Janssen H.M., de Waal B.F.M., Willard N.P., Meijer E. W., Grüll H., 2007. Dendritic PARACEST contrast agents for magnetic resonance imaging. Contrast Media Mol Imaging. 2: 229–239. Doi: 10.1002/cmmi.149

Revett T., Baker G., Jhamandas J., and Kar S., 2013. Glutamate system, amyloid β peptides and tau protein: functional interrelationships and relevance to Alzheimer disease pathology. J. Psychiatry Neurosci. 38 (1): 6-23.

Roussel T., Frydman L., Le Bihan D. and Ciobanu L., 2019. Brain sugar consumption during neuronal activation detected by CEST functional MRI at ultra-high magnetic fields. Sci. Rep. 9(1):4423. doi: 10.1038/s41598-019-40986-9.

Sagiyama K., Mashimo T., Togao O., Vemireddy V., Hatanpaa K.J., Maher E.A., Mickey B.E., Pan E., Sherry A.D., Bachoo .RM., Takahashi M., 2014. In vivo chemical exchange saturation transfer imaging allows early detection of a therapeutic response in glioblastoma. Proc Natl Acad Sci U S A. 111(12):4542-4547. doi: 10.1073/pnas.1323855111

Sehgal A.A., Li Y., Lal B., Yadav N.N., Xu X., Xu J., Laterra J., van Zijl P.C.M., 2019. CEST MRI of 3-O-methyl-D-glucose uptake and accumulation in brain tumors. Magn Reson Med. 81(3):1993-2000. doi: 10.1002/mrm.27489.

Shaffer J. J., Mani M., Schmitz S.L., Xu J., Owusu N., Wu D., Magnotta V.A., Wemmie J.A., 2020. Proton Exchange Magnetic Resonance Imaging: Current and Future Applications in Psychiatric Research. Front. Psychiatry. 11. doi : 10.3389/fpsyt.2020.532606

Sherry A.D. and Woods M., 2008. Chemical Exchange Saturation Transfer Contrast Agents for Magnetic Resonance Imaging. Annu. Rev. Biomed. Eng. 10:391–411.

Song X., Yang X., Ray Banerjee S., Pomper M. G. and McMahon M. T., 2015. Anthranilic acid analogs as diamagnetic CEST MRI contrast agents that feature an intramolecular-bond shifted hydrogen: Novel anthranilic acid IM-SHY diacest MRI agents. Contrast Media Mol. Imaging, 10(1): 74-80.

Sun P. Z., Zhou J., Sun W., Huang J., and van Zijl P. C. M., 2007. Detection of the ischemic penumbra using pH-weighted MRI. J. Cereb. Blood Flow Metab. 27(6): 1129-1136.

Togao O., Yoshiura T., Keupp J., Hiwatashi A., Yamashita K., Kikuchi K., Suzuki Y., Suzuki S.O., Iwaki T., Hata N., Mizoguchi M., Yoshimoto K., Sagiyama K., Takahashi M., Honda H., 2014. Amide proton transfer imaging of adult diffuse gliomas: correlation with histopathological grades. Neuro Oncol. 16(3):441-8. doi: 10.1093/neuonc/not158

Tolomeo D., Micotti E., Serra S.C., Chappell M., Snellman A., Forloni G., 2018. Chemical exchange saturation transfer MRI shows low cerebral 2-deoxy-D-glucose uptake in a model of Alzheimer's Disease. Sci Rep. 8(1):9576. doi: 10.1038/s41598-018-27839-7.

van Zijl P.C.M., Jones C.K., Ren J., Malloy C.R., Sherry A.D., 2007. MRI detection of glycogen in vivo by using chemical exchange saturation transfer imaging (glycoCEST). Proc Natl Acad Sci U S A. 104(11):4359-64. doi: 10.1073/pnas.0700281104.

van Zijl P. C. M. and Yadav N. N., 2011. Chemical exchange saturation transfer (CEST): What is in a name and what isn't? Magn. Reson. Med. 65(4): 927-948.

Wang J., Weygand J., Hwang K.P., Mohamed A.S., Ding Y., Fuller C.D., Lai S.Y., Frank S.J., Zhou J., 2016. Magnetic Resonance Imaging of Glucose Uptake and Metabolism in Patients with Head and Neck Cancer. Sci Rep. 6:30618. doi: 10.1038/srep30618.

Wang M., Hong X., Chang C.F., Li Q., Ma B., Zhang H., Xiang S., Heo H.Y., Zhang Y., Lee D.H., Jiang S., Leigh R., Koehler R.C., van Zijl P.C.M., Wang J., Zhou J., 2015. Simultaneous detection and separation of hyperacute intracerebral hemorrhage and cerebral ischemia using amide proton transfer MRI. Magn Reson Med. 74(1):42-50. doi: 10.1002/mrm.25690.

Wang R., Li S.Y., Chen M., Zhou J.Y., Peng D.T., Zhang C., Dai Y.M., 2015. Amide proton transfer magnetic resonance imaging of Alzheimer's disease at 3.0 Tesla: a preliminary study. Chin Med J (Engl). 128(5):615-619. doi: 10.4103/0366-6999.151658.

Ward K., Aletras A. and Balaban R., 2000. A New Class of Contrast Agents for MRI Based on Proton Chemical Exchange Dependent Saturation Transfer (CEST). J. Magn. Reson. 143(1): 79-87.

Ward K.M. and Balaban R.S., 2000. Determination of pH using water protons and Chemical Exchange dependent Saturation Transfert (CEST). Magn Reson Med. 44:799-802.

Wells J.A., O'Callaghan J.M., Holmes H.E., Powell N.M., Johnson R.A., Siow B., Torrealdea F., Ismail O., Walker-Samuel S., Golay X., Rega M., Richardson S., Modat M., Cardoso M.J., Ourselin S., Schwarz A.J., Ahmed Z., Murray T.K., O'Neill M.J., Collins E.C., Colgan N., Lythgoe M.F., 2015. In vivo imaging of tau pathology using multi-parametric quantitative MRI. Neuroimage. 111:369-378. doi: 10.1016/j.neuroimage.2015.02.023.

Wen Z., Hu S., Huang F., Wang X., Guo L., Quan X., Wang S., Zhou J., 2010. MR imaging of high-grade brain tumors using endogenous protein and peptide-based contrast. Neuroimage. 51(2):616-622. doi: 10.1016/j.neuroimage.2010.02.050.

Xu X., Chan K.W., Knutsson L., Artemov D., Xu J., Liu G., Kato Y., Lal B., Laterra J., McMahon M.T., van Zijl P.C., 2015. Dynamic glucose enhanced (DGE) MRI for combined imaging of blood-brain barrier break down and increased blood volume in brain cancer. Magn Reson Med. 74(6):1556-1563. doi: 10.1002/mrm.25995.

Xu X., Sehgal A.A., Yadav N.N., Laterra J., Blair L., Blakeley J., Seidemo A., Coughlin J.M., Pomper M.G., Knutsson L. and van Zijl P.C.M., 2019. d-glucose weighted chemical exchange saturation transfer (glucoCEST)-based dynamic glucose enhanced (DGE) MRI at 3T: early experience in healthy volunteers and brain tumor patients. Magn Reson Med. 24. doi: 10.1002/mrm.28124)

Yang X., Song X., Li Y., Liu G., Banerjee S.R., Pomper M.G., McMahon M.T., 2013. Salicylic acid and analogues as diaCEST MRI contrast agents with highly shifted exchangeable proton frequencies. Angew Chem Int Ed Engl. 52(31):8116-8119. doi: 10.1002/anie.201302764.

Yang Y., Qu X., Huang Y., Afsar K., Yan G., Guo G., Duan S., 2020. Preliminary application of 3.0 T magnetic resonance chemical exchange saturation transfer imaging in brain metastasis of lung cancer. BMC Med Imaging. 20(1):4. doi: 10.1186/s12880-019-0400-y.

Zaiss M., Schmitt B., Bachert P., 2011. Quantitative separation of CEST effect from magnetization transfer and spillover effects by Lorentzian-line-fit analysis of z-spectra. J Magn Reson 211(2):149–55. doi: 10.1016/j.jmr.2011.05.001

Zhang D., Li J., Wang F., Hu J., Wang S. and Sun Y., 2014. 2-Deoxy-D-glucose targeting of glucose metabolism in cancer cells as a potential therapy. Cancer Lett. 355(2): 176-183.

Zhang J., Yuan Y., Gao M., Han Z., Chu C., Li Y., van Zijl P. C. M., Ying M., Bulte J. W. M., Liu G., 2019. Carbon Dots as a New Class of Diamagnetic Chemical Exchange Saturation Transfer (diaCEST) MRI Contrast Agents. Angew Chem Int Ed Engl. 58(29):9871-9875. Doi: 10.1002/anie.201904722

Zhang, S., Winter, P., Wu, K., Sherry, A.D., 2001. "A novel europium(III)-based MRI contrast agent. The first demonstration of a paramagnetic CEST agent as a MRI agent." J. Am. Chem. Soc 123: 1517–1518. Doi.org/10.1021/ja005820q

Zhang S., Merritt M., Woessner D. E., Lenkinski R. E. and Sherry A. D., 2003. PARACEST Agents: Modulating MRI Contrast via Water Proton Exchange. Acc. Chem. Res. 36(10):783-790.

Zhao J.M., Har-el Y.E., McMahon M.T., Zhou J., Sherry A.D., Sgouros G., Bulte J.W., van Zijl P.C., 2008. Size-induced enhancement of chemical exchange saturation transfer (CEST) contrast in liposomes. J Am Chem Soc. 130(15):5178-84. doi: 10.1021/ja710159q

Zhou J., Lal B., Wilson D. A., Laterra J., and van Zijl P. C., 2003a. M. Amide proton transfer (APT) contrast for imaging of brain tumors. Magn. Reson. Med. 50(6): 1120-1126. DOI: 10.1002/mrm.10651

Zhou J., Payen J.F., Wilson D.A., Traystman R.J. and van Zijl P.C., 2003b. Using the amide proton signals of intracellular proteins and peptides to detect pH effects in MRI. Nat Med. 8:1085-1090. doi: 10.1038/nm907

Zhou, J., and van Zijl, P. C. M., 2006. Chemical exchange saturation transfer imaging and spectroscopy. Prog Nuc Magn Reson Spect 48(2-3), 109-136. https://doi.org/10.1016/j.pnmrs.2006.01.001

Zhou, J., Heo, H.-Y., Knutsson, L., van Zijl, P.C. and Jiang, S., 2019. APT-weighted MRI: Techniques, current neuro applications, and challenging issues. J. Magn. Reson. Imaging, 50: 347-364. https://doi.org/10.1002/jmri.26645

Figure 1

Principle of Chemical exchange saturation transfer (CEST): A, B: Solute exchangeable protons (blue) are saturated at their specific resonance frequency in the proton spectrum (here 8.25 ppm for amide protons). This saturation is transferred to water, after a period (t_{sat}), this effect becomes visible on the water signal (B, right). C: Measurement of normalized water saturation (S_{sat}/S_0) as a function of irradiation frequency, generating a so-called Z-spectrum (or CEST spectrum), with water assigned to 0 ppm. D: Result of magnetization transfer ratio (MTR = $1 – S_{sat}/S_0$) asymmetry analysis of the Z-spectrum with respect to the water frequency to remove the effect of direct saturation.
(From “Zijl and Yadav. Chemical Exchange Saturation Transfer (CEST): what is in a name and what isn’t? Magn. Reson. Med. 2011; 65(4): 927–948” figure 1 with the authorization of Wiley & Sons)

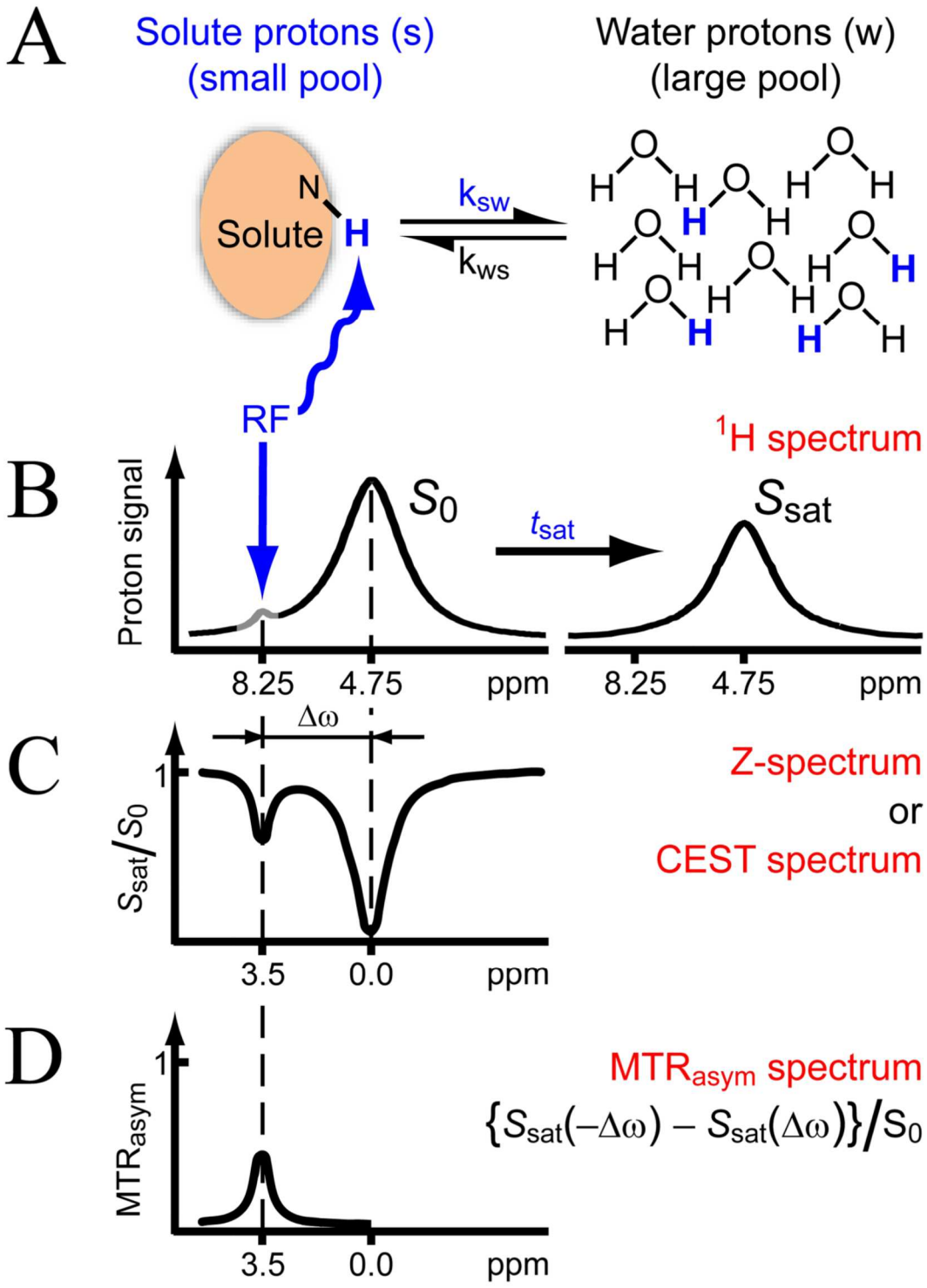
A
Solute protons (s)
(small pool)
Water protons (w)
(large pool)
N
Solute
H
k_{sw}
k_{ws}
RF
B
^{1}H spectrum
Proton signal
S_0
t_{sat}
S_{sat}
8.25
4.75
ppm
8.25
4.75
ppm
C
Δω
1
S_{sat}/S_0
Z-spectrum
or
CEST spectrum
3.5
0.0
ppm
D
1
MTR_{asym}
MTR_{asym} spectrum
$\{S_{sat}(-\Delta\omega) - S_{sat}(\Delta\omega)\}/S_0$
3.5
0.0
ppm

Figure 2

Different slices of relaxation-compensated CEST MRI of a patient with newly diagnosed glioblastoma grade IV, a central nervous system tumor, examined at 3T. The tumor volume can be seen in the coregistered gadolinium contrast enhanced T1-weighted images. The CEST-MRI MTRRex (taking into account water relaxation properties R1 and R2) and AREX (compensation for the scaling of all CEST effects by the T1 relaxation of water) images of the individual CEST signals of APT (Amide Proton Transfert) and rNOE (relayed Nuclear Overhauser Effect) showed distinct changes in the tumour region, highlighting several different morphological features The pink arrows indicate a hyperintense region, which most likely corresponds to a blood clot within the tumor.

(From "Goerke et al. Relaxation-compensated APT and rNOE CEST-MRI of human brain tumors at 3T. Magn Reson Med. 2019. 82(2):622-632" figure 6 with the authorization of Wiley & Sons)

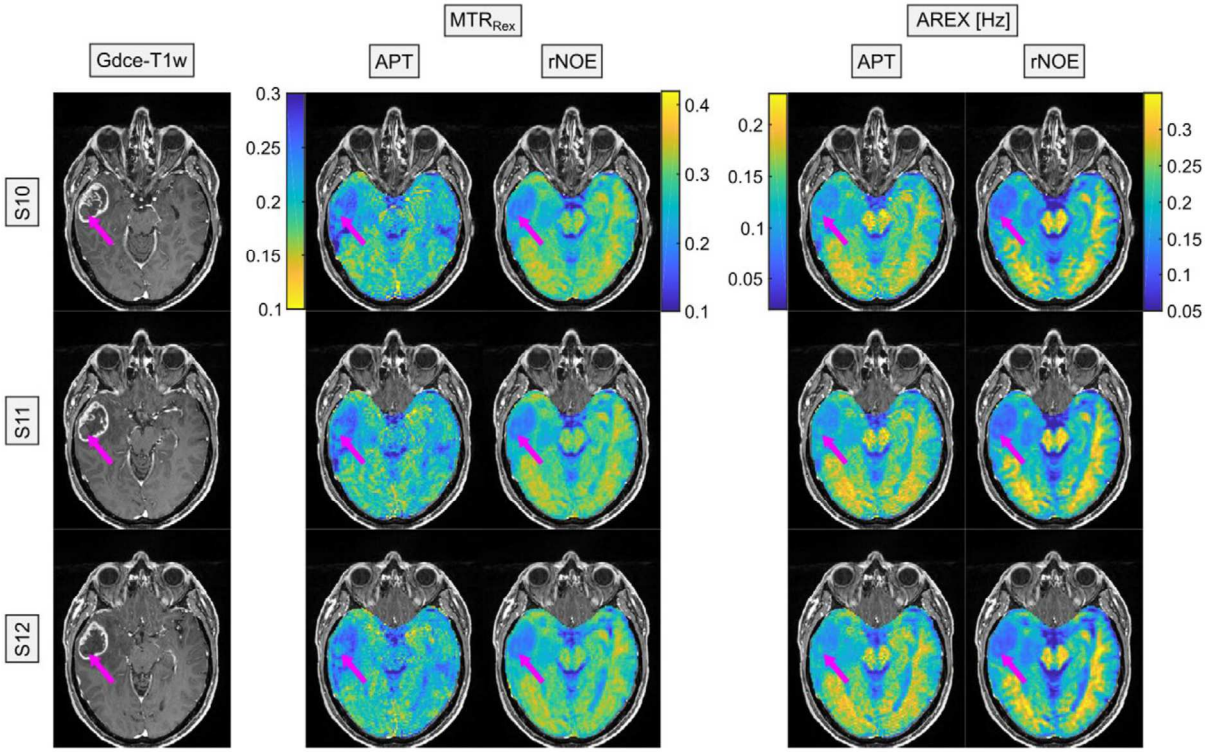

Table of different endogenous molecules used in neuroimaging *via* CEST

Technique	*CEST agents*	*Chemical groups*	*Chemical Shift*	*Application*	*References*
APT	*Mobile proteins and peptides*	*Amide (-NH)*	*~3,5 ppm*	*Strokes (ischemic and hemorrhagic) Tumors Neurodegenerative diseases*	*Chen et al 2019 ; Choi et al, 2018; Harston et al, 2015 ; Hectors et al, 2014 ; Holmes et al, 2016; Jeong et al, 2017 ; Jiang et al, 2016 ; Jones et al, 2006 ; Law et al, 2018 ; Li et al, 2014; 2017 ; Ma et al, 2017 ; Sagiyama et al, 2014 ; Sun et al 2007 ; Togao et al, 2014; Wang et al, 2015 ; Wells et al, 2015 ; Wen et al 2010 ; Yang et al 2020 ; Zhou et al 2003a ; Zhou et al, 2003b*
GluCEST	*Glutamate*	*Amine (-NH2)*	*~3 ppm*	*Neurodegenerative diseases, monitoring,*	*Bagga et al, 2016; Cai et al 2013; Cai et al, 2012 ; Crescenzi et al, 2014, 2017; Davis et al, 2015; Flament et al, 2018; Haris et al, 2013a; Haris et al., 2014a; Haris et al., 2014b; Kostic et al, 2013; Lee et al 2019a; Lee et al, 2019c ; Mao et al, 2019; O'Grady et al, 2019; Pépin et al, 2016; Revett et al, 2013.*
GlucoCEST	*Glucose*	*Hydroxyl (-OH)*	*3 peaks [1.2 / 2.2/ 2.8 ppm]*	*Tumors*	*Chan et al, 2012; Nasrallah et al, 2013; Roussel et al, 2019; Sehgal et al, 2019; Wang et al, 2016; Xu et al 2015; Xu et al, 2019; Zhang et al, 2014.*
MICEST	*Myo-inositol*	*Hydroxyl (-OH)*	*3 peaks [0.8 / 0.9 / 1.1 ppm]*	*Neurodegenerative diseases*	*Fisher et al, 2002 Haris et al, 2011 Haris et al, 2013b*
CrCEST	*Creatine*	*Amine (-NH2)*	*~1.8 ppm*	*Tumors, seizures*	*Cai et al, 2015; Cai et al, 2017; Haris et al,*

					2012; Joncquel-Chevalier Curt et al, 2015; Kogan et al, 2014; Lee et al, 2019b.